TOPOLOGICAL ANALYSIS OF WALL MASS TRANSPORT USING A LUMINESCENT IMMOBILIZED ENZYMATIC SYSTEM

MAURICE NAKACHE
Institut National de la Santé et de la Recherche Médicale/E.R.A. Centre National de la Recherche Scientifique 785, Hôpital Broussais, 75674 Paris, Cedex 14, France

JEAN-LUC DIMICOLI
Unité 219 Institut National de la Santé et de la Recherche Médicale, Institut Curie, Section de Biologie, Centre Universitaire, 91405 Orsay, France

ABSTRACT A new technique of visualization of diffusion-convection phenomena at a solid-liquid interface using the luminol chemiluminescent reaction catalyzed by immobilized peroxidase has been previously described (Dimicoli, J. L., M. Nakache, and P. Peronneau, 1982, *Biorheology*, 19:281–300). We propose now a theoretical model that predicts quantitatively the light fluxes, J_L, corresponding to the transfer J of the hydrogen peroxide substrate at the liquid-solid interface in a cylindrical tube for continuous flow experiments. A simple phenomenological relation, $J \propto J_L^{1/m}$ ($1 < m < 3$) was first established for each point of the wall. Then, numerical integration showed that, independent of the laminar or turbulent character of the flow, $J_L^{1/m}$ was proportional to $(S1\ K_{ideal})/(1 + K_{ideal}/ET)$, where $S1$ is the bulk substrate concentration, K_{ideal} is the ideal transport coefficient, and ET (in $cm \cdot s^{-1}$) a phenomenological first-order enzymatic rate constant per unit of wall surface. This relation proved to be satisfactory for all experimental conditions since a single mean value of ET takes into account the experimental data collected for a given enzymated tube in a large range of Reynolds number values (Re) ($500 < Re < 9{,}000$) and of distances from the entrance of the tube ($x > 0.3$ cm). This quantitative analysis using a pseudo–first-order approximation interprets the observed great dependence of J_L on Re($J_L \propto Re^{n'}$, with n' usually $>1/3$ for laminar flows) and on $S1$ ($J_L \propto S1^m$). It predicts also that the laminar-to-turbulent transition can be evidenced for interfacial enzymatic activity, $ET > 2.10^{-4}$ $cm \cdot s^{-1}$, as observed with most of the tubes prepared by covalent binding of peroxidase on the acrylamide gel wall. The experiment had to be carried out at a pH value of 8, which correponds to the fastest rate of the chemiluminescent reaction. The predicted entrance effects were also observed experimentally for the first time in an immobilized enzyme system. This technique appears therefore to be a valuable tool for the quantitative analysis of diffusion-convection phenomena at a liquid-solid interface with a good spatial resolution with a great range of flow rate.

INTRODUCTION

A new methodological approach for the investigation of diffusion-convection phenomena at a solid-liquid interface using immobilized enzymes was previously proposed (1). It is based on several investigations (1–6) that show that the consumption of a substrate dissolved in the flowing liquid phase could be limited by the diffusion-convection transport of the substrate from the liquid phase to the wall if the enzymatic reaction is sufficiently rapid. We have then selected (7) an enzyme that catalyzes a chemiluminescent reaction, i.e., the oxidation of luminol by hydrogen peroxide catalyzed by horseradish peroxidase (8, 9). It was thus possible to measure the product of the reaction, light, at any position along the wall. This was a considerable improvement over other enzymatic reactions with products dissolved in the liquid phase. Under such conditions, only integrated fluxes over the whole wall are accessible and no topological data are available.

By entrapping peroxidase in the pores of a layer of polyacrylamide gel coating a transparent glass tube, it was possible to measure the light flux, J_L, as a function of the flow rate at any position along the wall. The measured values of J_L were then in qualitative agreement with theoretical values predicted for systems in which diffusion-convection control occurs (7). However, this control did not appear very high and, particularly, the laminar-to-turbulent transition, which should lead to an important increase of substrate transport to the wall at high reaction yield (10, 11), was never observed.

The use of this method in more complex situations, such as in time-dependent flows or in geometries that are not

Address all correspondence to Jean-Luc Dimicoli.

cylindrical, requires both technical improvements and quantitative analysis. We describe now an improved method of enzyme immobilization that leads to high surface activities and thus to a greater sensitivity to diffusion-convection phenomena. The experimental data are then interpreted quantitatively in terms of both substrate diffusion convection at the wall and reaction rate in the gel.

MATERIALS AND METHODS

Immobilized Enzymatic Systems

Horseradish peroxidase (8, 9) was immobilized using two different methods. The first one, already described (7), involves noncovalent entrapment of the protein within polyacrylamide–gel-walled glass tubes. The second one involves covalent binding of the protein at the surface of the gel-walled tubes and results in higher enzymatic activities.

10 mm outside diameter, 7 mm inside diameter, and 140 mm long Pyrex glass tubes were incubated for 1 h in a 4% solution of silane A174 (Pharmacia Fine Chemicals Div. of Pharmacia Inc., Piscataway, NJ) in aqueous acetic acid, pH 3.5. A rod of polymethyl methacrylate, 6 mm in diameter and 150 mm long, was inserted coaxially in the tube and the resulting annulus, closed at the bottom, was filled with the required solutions. For the entrapment method, this solution was a 0.2 M $NaOH-H_3BO_3$ buffer, pH 9, containing 10^{-3} M luminol, 8.5% acrylamide, 1.5% *N-N'*-diallyltartardiamide, and 0.5 g/l EDTA to eliminate traces of metals that could directly catalyze the luminol reaction and produce a background light signal (all chemicals were obtained from Aldrich Chemical Co. Inc., Milwaukee, WI). Horseradish peroxidase (E.C. 1.11.1.7; Boehringer Mannheim Biochemicals, Indianapolis, IN) was added at a concentration of 8 mg/ml. For the covalent binding method, the solution was a 0.15 M phosphate buffer, pH 7.5, containing 8.5% acrylamide and 1.5% *N-N'*-diallyltartardiamide.

In both cases, the polymerization and the covalent binding of the polyacrylamide gel on the glass (12) were carried out photochemically under anaerobic conditions using a mercury lamp, after addition of 1 mg/ml of riboflavin and of ammonium persulfate. In the first method, the smooth gel-walled tubes obtained after polymerization had an inside diameter of 5.6 mm and were thoroughly washed with the luminol buffer solution before use. For covalent binding of the protein, the gel surface was incubated overnight at 37°C using a 10% glutaraldehyde solution in 0.15 M phosphate buffer (15), then washed with the pure buffer. The tubes were then filled during a 24 h period at 25°C with a 4 mg/ml enzyme solution and finally washed thoroughly with the buffer before use.

All experiments were carried out with luminol in great excess (10^{-3} M), with respect to hydrogen peroxide ($\sim 5 \times 10^{-5}$ M), in 0.2 M $KOH-H_3BO_3$ buffer, pH 8 or 9. The reaction thus depended only on the H_2O_2 concentration (measured by the method of Cotton and Dunford [14]), the luminol concentration remained constant throughout the experiments.

Hydrodynamical Circuit

The hydrodynamical set up is presented in Fig. 1. An enzymated tube was inserted vertically between two 1 meter long glass tubes of 7 mm inside diameter using short plastic muffs (80 mm long, 7 mm outside diameter, 5.6 mm inside diameter) to minimize the stenotic effect due to the reduction of the internal diameter (7 to 5.6 mm) due to the enzymated gel (see below). The continuous flow of substrate solution, activated up to 3 l per minute by a peristaltic pump, went through two upstream stabilizers to eliminate any periodical source of noise. According to the theory of Krindel and Silberberg (15) and to our own calculations (7), the characteristics of the flow in the gel-walled tubes should not depend significantly upon the presence of the gel. We may thus assume that the flow through the tubes is identical to that in rigid cylindrical tubes of 5.6 mm inside diameter.

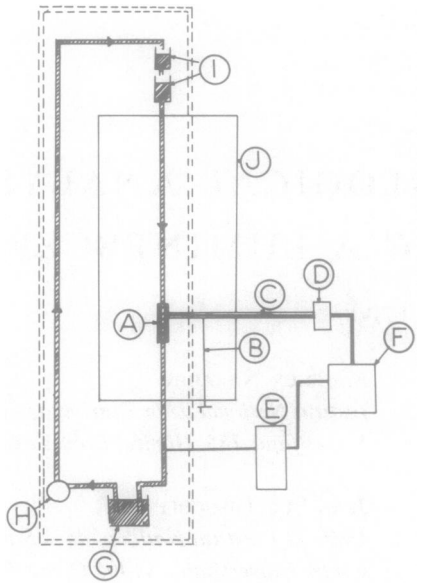

FIGURE 1 The experimental set up. *A*, enzymated tube; *B*, handle for positioning the optical fiber; *C* and *D*, photomultiplier; *E*, electromagnetic flowmeter; *F*, cathodic screen; *G*, 1.5-l substrate bath; *H*, peristaltic pump; *I*, flow stabilizers; *J*, blackbox. The double line indicates the hydrodynamical circuit; the strong single line indicates the measurement system.

Measurements of the Velocity Profiles of the Flowing Liquid

To verify that the stenotic effect was adequately reduced using the 80 mm long plastic muffs, we measured the water-velocity profiles using a homemade pulsed-type Doppler velocimeter operating at 15 MHz (0.1-mm spatial resolution). This requires the presence of particles (in our case, wheat starch) in the liquid flow for the backscattering of the ultrasonic waves. The equipment and the method have already been described (16). We verified that the velocity profiles and thus the velocity gradient at the wall do not depend on the position along the tube for distances to the stenose >5 cm. This shows that the flow was well developed in the enzymated tube and that the stenotic effect due to the presence of the gel was adequately reduced.

Light-Flux Measurements and Data Acquisition

An optical glass fiber (3.2 mm diam, 0.5 m long, and 60° acceptance angle, from Oriel Corp. of America, Stanford, CT) could be moved along the tube, using a mobile arm. This corresponded to a light emission rate measurement with a space resolution of ~5 mm. The transmittance of the glass fiber at 420 nm was 50%. The current of a photomultiplier (R928; Hamamatsu Corp., Middlesex, NJ) operated at 900 V and placed at the output of the fiber was amplified ($\times 10^8$ to 10^9) by a fast picoammeter, then recorded on an oscilloscope. The signal of the flow meter was recorded simultaneously. The zero levels were obtained by stopping the flow for a few seconds.

RESULTS

Two types of experiments have been carried out: (*a*) the measurement of the total light flux, J_L, as a function of the

H_2O_2 concentration, $S1$, for fixed values of the mean flow velocity, C_m, and of the distance, x, from the input of the tube; (*b*) the measurement of J_L, at a fixed concentration $S1$, as a function of x and of the Reynolds number, Re, defined as $Re = 2rC_m/\nu$ where r and ν are the radius of the tube and the kinematic viscosity of water. ν was kept constant (pure water) and C_m varied.

Dependence of J_L on the H_2O_2 Concentration $S1$

For a given tube and pH value, J_L, is always proportional to $S1^m$, with m almost independent of x and Re for $S1 < 1.5 \times 10^{-4}$ M. The largest variations of m for a given tube never exceeds ±10% and m is always >1 and in most cases >1.5. Comparable observations for similar enzyme configuration have already been published (8).

Dependence of J_L on Re and x

These new experimental data confirm our first observations (7) since J_L is dependent on both Re and x. Fig. 2 summarizes data obtained with a tube prepared by covalent binding of the enzyme and suggests already that the surface activity for this kind of preparation is higher than that in the tubes obtained by enzyme entrapment (7). Now, the laminar-to-turbulent transition is clearly observable for Re values ~2,500 and sufficiently large x values.

A quantitative analysis of the data is presented in Tables I and II. The light-flux intensity was analyzed as a function of the Reynolds number by nonlinear fitting to $J_{Lo}Re^{n'}$. J_{Lo} was arbitrarily chosen for each tube as the light flux for Re equals 500 (laminar flows) or 2,500 (turbulent flows) at each x value, usually 0.3 and 3.3 cm. The n' value thus depends on the mode of enzyme fixation, the x position along the tube, and the laminar or turbulent nature of the flow.

In laminar conditions the value of n' for $x = 3.3$ cm is always greater than that for $x = 0.3$ cm. This effect is not

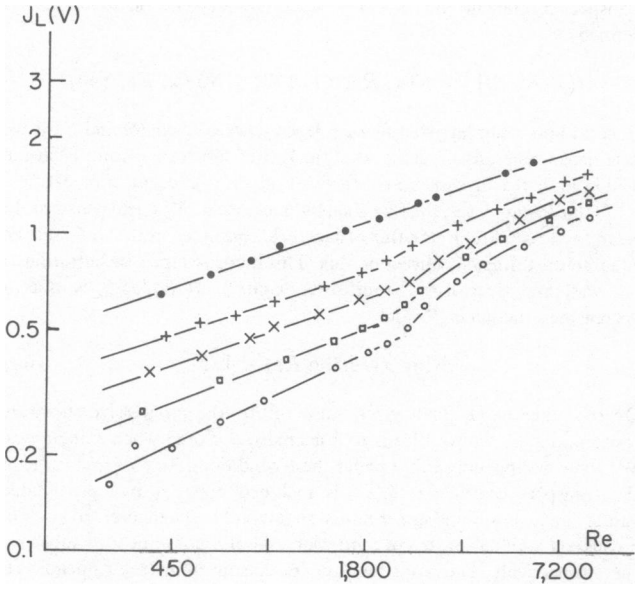

FIGURE 2 Effect on Re on J_L as a function of x for a tube obtained by covalent binding to the enzyme running at pH 8. The values of x are the following: (●) 0.3 cm, (+) 1.3 cm, (x) 2.3 cm, (□) 3.3 cm, and (○) 4.3 cm.

TABLE I
EFFECT OF H_2O_2 CONCENTRATION $S1$ ON THE n' VALUES* OBTAINED FROM THE EQUATION $J_L = J_{Lo}Re^{n'}$

$S1$	n'_1	n'_2	n'_3	n'_4
5.6×10^{-5} M	0.255 (0.02)‡	0.182 (0.004)	0.330 (0.028)	0.365 (0.010)
8.4×10^{-5} M	0.245 (0.015)	0.181 (0.012)	0.316 (0.017)	0.346 (0.016)
1.4×10^{-4} M	0.237 (0.01)	0.150 (0.006)	0.311 (0.01)	0.283 (0.033)

*The n' values are obtained from the data corresponding to $Re < 2{,}000$ and $x = 0.3$ cm (n'_1), $Re > 2{,}000$ and $x = 0.3$ cm (n'_2), $Re < 2{,}000$ and $x = 3.3$ cm (n'_3), and $Re > 2{,}000$ and $x = 3.3$ cm (n'_4), pH 8.
‡The numbers in parentheses are the standard deviation of n' obtained by nonlinear regression analysis.

TABLE II
RESULTS OF THE ANALYSIS OF $J_L = J_{Lo}Re^{n'}$ IN DIFFERENT CONDITIONS AND FOR DIFFERENT TUBES

Tube number	Mode of preparation‡	pH	x	N_{lam}*	n'_{lam}	N_{turb}	n'_{turb}	m‖
1	I	8	0.3	7	0.340 (0.014)§	6	0.344 (0.024)	1.6
1	I	8	3.3	6	0.405 (0.02)	8	0.541 (0.031)	
2	I	8	0.3	11	0.255 (0.02)	6	0.182 (0.04)	1.4
		8	3.3	8	0.330 (0.028)	6	0.365 (0.010)	
2	I	9.5	0.3	6	0.164 (0.006)	6	0.091 (0.009)	2.2
		9.5	3.3	6	0.324 (0.026)	8	0.076 (0.037)	
3	II	8	0.3	5	0.220 (0.01)	6	0.224 (0.025)	1.7
		8	3.3	7	0.350 (0.01)	6	0.376 (0.036)	

*N_{lam} and N_{turb} are the number of data points used to perform the nonlinear regression analysis in laminar ($Re < 2{,}100$) and turbulent flows ($Re > 2{,}100$), respectively.
‡Modes of preparation I and II are the covalent binding and the entrapment, respectively.
§Values in parentheses are standard deviations obtained from the nonlinear regression analysis.
‖m is the coefficient in the relation of the light flux, J_L, with the hydrogen peroxide substrate concentration $S1$, $J_L \alpha S1^m$.

due to an heterogenous enzymatic activity. For example, when the tube 2 in Table II is turned over and the optical fiber positioned at the former input of the tube, corresponding now to the output of the tube, the value of n' is 0.33 instead of 0.16 pH 9.5. The increase of n' when the laminar-to-turbulent transition occurs is always much higher at $x = 3.3$ cm than at $x = 0.3$ cm. A decrease of n' is even observed at $x = 0.3$ cm for the tube 2 operated at pH 9.5.

The dependence of J_L on the Reynolds number is a function of $S1$ only if $S1 > 10^{-4}$ M. Table I and Fig. 3 show for $S1 = 1.4 \times 10^{-4}$ M, a smaller value of n', particularly at $x = 3.3$ and for turbulent flows.

For laminar flows, most of the tubes exhibit at 3.3 cm large n' values equal to or higher than 1/3, a value expected for an indeal transport of substrate to the wall (see below and [17]). This observation could appear contradictory with that of large values for the order m characterizing the dependence of J_L on $S1$. In fact, if the transport was ideal, the flux of substrate J should be proportional to $S1$. A quantitative interpretation of the data should solve this apparent contradiction by providing the relation between J and J_L. This should require taking into account the mechanism of light emission.

THEORY

The values and relationships of J, the flux of substrate, and J_L, the light-emission flux, should depend on the characteristics of both the diffusion-convection phenomena and the enzymatic reaction. This will be developed in three steps. (*a*) The substrate transfer at the wall of a cylindrical tube, where it is consumed by a chemical reaction, will be considered comparing just the ideal case with more actual situations where the substrate concentration at the wall is not zero. (*b*) We shall then consider the present enzymatic system responsible for a complex relation between J and J_L, and look for an appropriate approximation for the diffusion of the reaction products and for the flux J. The relationship between J and J_L, so established, will be better substantiated for fast experimental conditions controlled more by diffusion; (*c*) finally, we shall describe a method for the estimation of the degree of diffusion control from the J data derived in the previous step. This will result from first-order phenomenological models fitting the experimental data.

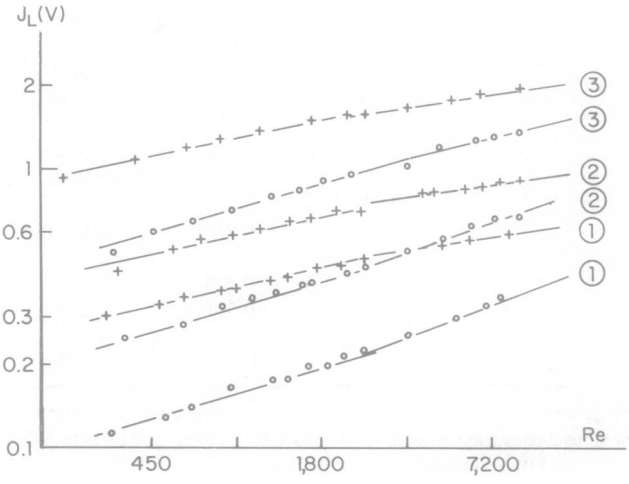

FIGURE 3 Effect of the H_2O_2 bulk concentrations S_1 on the dependence of J_L on Re for a tube obtained by covalent binding to the enzyme and running at pH 8. For each H_2O_2 concentration (5.6×10^{-5}, [1], 8.4×10^{-5} [2], and 1.4×10^{-4} M [3]) log J_L is given at two positions on the tube ($x = 0.3$ [+] and 3.3 cm [o]).

Diffusion Convection of a Substrate at a Liquid-Solid Interface

We shall consider a laminar flow of a substrate solution in a cylindrical tube having a radius, r, large enough so that the diffusion layer, where the substrate concentration, S, changes between its values at the interface $S0$ and $S1$ in the bulk solution, is negligible as compared with r. We shall show that this is actually the case under our experimental conditions. The problem may then be reduced to two dimensions, x and y, parallel and perpendicular to the flow. The velocity of the liquid at the position y in the diffusion layer is simply Gy, where G is the velocity gradient at the wall. For laminar flows $G = 4\ C_m/r$, C_m being the mean flow velocity. The substrate concentration profile in the liquid phase is given by

$$D_{LS}\frac{\partial^2 S}{\partial y^2} - \frac{4C_m y}{\nu}\frac{\partial S}{\partial X} = 0; \quad x > 0, y > 0, \tag{1}$$

$$S0 = S0(x); \quad x > 0, y = 0, \tag{2}$$

where D_{LS} is the diffusion coefficient of the substrate in the liquid phase. The boundary condition (Eq. 2) describes the steady state interfacial concentration such that at each point of the interface

$$D_{LS}\left(\frac{\partial S}{\partial y}\right)_{y=0} = J(S0), \tag{3}$$

where $J(S0)$ is the flux of substrate consumed at the wall and $D_{LS}(\partial S/\partial y)_{y=0}$ is the flux of substrate due to diffusion convection to the interface. When the reaction is very fast, $S0$ is very small and negligible for any value of x. The substrate flux is then ideal, and by integration (17)

$$J_{ideal}^{(x,RE)} = K_{ideal}^{(x)} S1 = 0.67\, D_{LS}^{2/3} x^{-1/3} r^{-2/3} \nu^{1/3} Re^{1/3} S1. \tag{4}$$

If $S0$ is no longer negligible as compared with $S1$, the effective transport coefficient $K(x, Re, S1)$ which now depends on Re and $S1$ is defined by

$$J(x, Re, S1) = K(x, Re, S1)\,[S1 - S0\,(x, Re, S1)]. \tag{5}$$

General limits can be given for the dependence of J on Re and $S1$ if we assume, as generally observed, that the flux of substrate consumed at the wall is an increasing function of the wall substrate concentration $S0$.

When Re increases, the flux J should increase if $S0$ is held constant. In steady state conditions, the flux of substrate consumed at the wall must be equal to the diffusion convection flux. This increases the concentration at the wall and decreases the diffusion control. $J(Re)/J_{ideal}^{(Re)}$ is thus a decreasing function of Re and

$$\partial(\log J)/\partial(\log Re) < 1/3. \tag{6a}$$

On the other hand, for a given value of Re, the progressive substrate consumption at the wall leads to a decrease of $S0(x)$ when x increases. We show in Appendix I that under these conditions the observed value of the transport coefficient, $K(x)$, is included between two predictable values. These lower and upper limits correspond to the theoretical cases of a constant wall substrate concentration and of a constant wall substrate flux, respectively. The limits for $J(x)$ are thus given by (see Appendix I)

$$K_{ideal}(x)\,[S1 - S0(x)] \le J(x) < 1.2\,K_{ideal}(x)\,[S1 - S0(x)]. \tag{6b}$$

If $S0(x)$ is not too large, $J(x)$ is almost proportional to $S1$ within an error of $1.2\ S0(x)/S1$.

Immobilized Peroxidase

There are at least two differences from the above ideal case for immobilized peroxidase: (*a*) the enzyme lies in a thick gel layer rather than on an infinitely thin layer at the interface; and (*b*) the flux of product, J_L, is observed rather than the flux, J, of substrate. The nature of the luminescent reaction must thus be considered to correlate the two fluxes for an enzyme in solution and for immobilized peroxidase. The latter situation should underline the role of the diffusion of intermediates in the reaction and large apparent orders of reaction, measured by J_L, should appear experimentally. We shall define afterwards the conditions in which a large dependence of J_L on Re must provide a simple relation between J_L and J.

Chemiluminescent Reaction in Solution. Cormier and Prichard (9) showed by stopped-flow experiments that enzymatically induced chemiluminescent reaction could be described by the following equations

$$\begin{aligned}
&E + H_2O_2 \xrightarrow{k_1} C_1 && (\alpha)\\
&C_1 + LH_2 \xrightarrow{k_2} C_2 + LH^{\cdot} && (\beta)\\
&C_2 + LH_2 \xrightarrow{k_3} E + LH^{\cdot} && (\gamma)\\
&2\,LH^{\cdot} + H_2O_2 \xrightarrow{k_4} h\nu + P && (\delta)
\end{aligned} \qquad (7)$$

where E, LH_2, and $LH^{\cdot}$ stand respectively for peroxidase, luminol, and the oxidized luminol radical. These authors confirmed experimentally the second order of the light emitting reaction (7).

Under steady state conditions where the H_2O_2 concentration and that of other intermediates may be considered as constant, $dC_1/dt = dC_2/dt = d[LH^{\cdot}]/dt = 0$. If the hydrogen peroxide concentration is high enough to assume a constant overall rate, then the rate of production of the luminol radical is

$$V^P_{LH^{\cdot}} = \frac{2k_1k_2k_3\,[E]\,[LH_2]\,[H_2O_2]}{k_2k_3\,[LH_2] + (k_1k_3 + k_1k_2)\,[H_2O_2]}, \qquad (8)$$

and the rate of consumption of $LH^{\cdot}$ in the chemiluminescent reaction is

$$V^C_{LH^{\cdot}} = 2\,k_4[H_2O_2][LH^{\cdot}]^2. \qquad (9)$$

since in steady conditions $V^C_{LH^{\cdot}} = V^P_{LH^{\cdot}}$
then,

$$[LH^{\cdot}] = \left(\frac{k_1k_2k_3[E]\,[LH_2]}{k_4\{k_2k_3[LH_2] + (k_1k_3 + k_1k_2)\,[H_2O_2]\}}\right)^{1/2}. \qquad (10)$$

The light emission flux, J_L, which is proportional to $[H_{20}O_2]\,[LH^{\cdot}]^2$ (Eq. 7), exhibits a simple phenomenological Michaelian dependence on $[H_2O_2]$ since $[LH_2]$ is constant in the presence of a large excess of luminol. The dependence of J_L on $[H_2O_2]$ cannot give any indication of the existence of chemical intermediates other than the eventual enzyme-substrate complexes in the process of light production. It will be shown below that this is no longer the case for immobilized enzymes.

Chemiluminescent Reaction in the Gel. Concentration gradients of any chemical species should appear in the immobilized enzyme systems, even if the concentration of peroxidase in the gel is uniform. The concentration profiles in the gel of the substrate H_2O_2 and of intermediate products such as $LH^{\cdot}$ radicals have to be established. We suppose for laminar flows that the problem can be reduced to two dimensions, as presented above for a smooth tube, and that the position-dependent concentration of the substrate S is low enough. Then $V^P_{LH^{\cdot}} \simeq 2\,k'S$ where $k' = k_1\,[E]$ according to Eq. 8.

The bulk diffusion equations in the gel for the hydrogen peroxide concentration (S) and the $LH^{\cdot}$ radical intermediate concentration (T) and then

$$D_{MS}\frac{\partial^2 S}{\partial y^2} - k'S - k_4T^2S = 0 \qquad (11a)$$

$$D_{MT}\frac{\partial^2 T}{\partial y^2} + 2k'S - 2k_4T^2S = 9, \qquad (11b)$$

where D_{MS} and D_{MT} are the diffusion coefficients in the gel of H_2O_2 and $LH^{\cdot}$, respectively.

The corresponding equations in the liquid phase are

$$D_{LS}\frac{\partial^2 S}{\partial y^2} - \frac{4yC_m}{r}\frac{\partial S}{\partial x} - k_4T^2S = 0 \qquad (12a)$$

$$D_{LT}\frac{\partial^2 T}{\partial y^2} - \frac{4yC_m}{r}\frac{\partial T}{\partial x} - 2k_4T^2S = 0, \qquad (12b)$$

where D_{LS} and D_{LT} are the diffusion coefficients in water and assuming that k_4 has the same values in both phases.

The boundary conditions are the following. At the gel-water interface

$$D_{LS}\left(\frac{\partial S}{\partial y}\right)_{0+} = D_{MS}\left(\frac{\partial S}{\partial y}\right)_{0-} \qquad (13a)$$

$$D_{LT}\left(\frac{\partial T}{\partial y}\right)_{0+} = D_{MT}\left(\frac{\partial T}{\partial y}\right)_{0-} \qquad (13b)$$

preventing any accumulation at the interface. (*b*) At the gel-glass interface

$$D_{MS}\left(\frac{\partial S}{\partial y}\right)_{y=-e} = 0 \qquad (14a)$$

$$D_{MT}\left(\frac{\partial T}{\partial y}\right)_{y=-e} = 0, \qquad (14b)$$

for a gel thickness e, since no flux can occur in the y direction at this interface as well as at the axis of the tube ($y = r$),

$$D_{LS}\left(\frac{\partial S}{\partial y}\right)_{y=+r} = 0 \qquad (15a)$$

$$D_{LT}\left(\frac{\partial T}{\partial y}\right)_{y=+r} = 0. \qquad (15b)$$

This complex system of differential equations (Eqs. 11–15) can hardly be integrated. It permits, however, some remarks on the apparent order on the light flux J_L relative to the bulk H_2O_2 concentration $S1$ and on the apparently too large dependence of $\log J_L$ upon $\log Re$.

Order of J_L Relative to $S1$. Two limiting cases for the diffusion $LH^{\cdot}$ simplify the bulk diffusion equations. (*a*) When the diffusion of $LH^{\cdot}$ is very slow in the gel, $D_{MT}(\partial^2T/\partial y^2)$ is negligible. The situation is then comparable with that in solution since the fate of each $LH^{\cdot}$ molecule does not depend on its vicinity, and the effects of concentration gradients can be omitted. Then, $T = (k'/k_4)^{1/2}$ and does not depend

on S, which is small. No LH· molecule can diffuse in the liquid phase and $k_4 T^2 S = 0$ in Eq. 12. The system of bulk equations is then

$$D_{MS} \frac{\partial^2 S}{\partial y^2} - 2k'S = 0 \tag{16}$$

$$D_{LS} \frac{\partial^2 S}{\partial y^2} - \frac{4yC_m}{r} \frac{\partial S}{\partial x} = 0 \tag{17}$$

for S, and

$$T = [k'/k_4]^{1/2} \tag{18}$$

$$T = 0 \tag{19}$$

for T, in the gel and in the liquid phases, respectively. The light flux, J_L, is proportional to $\int_{-e}^{r} k_4 T^2 S \, dy$ and thus to $\int_{-e}^{0} k'S \, dy$. The system of equations is linear in S, and S and J_L should be proportional to the bulk H_2O_2 concentration $S1$ with an apparent order of 1.

(*b*) When the diffusion of LH· is fast both in the gel and in water, T is small and $k_4 T^2 S$ is negligible as compared with the other terms. The system of bulk equations is thus reduced to

$$D_{MS} \frac{\partial^2 S}{\partial y^2} - k'S = 0 \tag{20}$$

$$D_{LS} \frac{\partial^2 S}{\partial y^2} - \frac{4yC_m}{r} \frac{\partial S}{\partial x} = 0 \tag{21}$$

for S, and

$$D_{MT} \frac{\partial^2 T}{\partial y^2} + 2k'S = 0 \tag{22}$$

$$D_{MS} \frac{\partial^2 T}{\partial y^2} - \frac{4yC_m}{r} \frac{\partial T}{\partial x} = 0 \tag{23}$$

for T, in the gel and liquid phases, respectively. This system is still linear in S and the profile of H_2O_2 concentration should be proportional to the bulk concentration $S1$. It is also linear for T and Eq. 22 indicates that T must also be proportional to $S1$. The light flux is still proportional to $\int_{-e}^{0} k_4 T^2 S \, dy$ and should appear proportional to $S1^3$, corresponding to an order of 3, since both T and S are proportional to $S1$.

In the general intermediate case, one could observe experimentally a light flux, J_L, proportional to $S1^m$ with $1 \le m \le 3$. Orders >2 have been observed in the present work and by others (8). It is interesting that the highest order of 2.35 observed by these authors was obtained for an enzyme solution separated from the substrate bath by a dialysis membrane. This order of reaction does not require 2 substrate molecules, as claimed by these authors (8), but rather 2 molecules of the intermediate product LH·. In general, the largest values of m will be observed for the largest diffusion velocity of LH· in the enzymated phase.

The existence of a step involving the reaction of H_2O_2 and LH· is evidenced with the immobilized enzyme through the high apparent order of the light emission reaction due to gradients of concentrations of the reactants in the sample. This is not the case in homogeneous solution and, as shown above, simple Michaelian kinetics is observed. Only time-dependent experiments, such as stopped flow measurements, can evidence the chemiluminescent step in solution. The immobilized enzyme thus reveals more clearly the detailed nature of the chemiluminescent process than the reaction in solution.

Dependence of J_L on Re and the Relation of the Substrate and Light Fluxes. One may assume that the reactions are mainly controlled by diffusion when the apparent dependence of J_L on Re is large. The substrate concentration at the interface $S0$ is then low as compared with $S1$ and the flux of substrate, J, is almost proportional to $S1$ (within a precision of the order of $S0/S1$, see Eq. 6b). The light flux, J_L, is thus proportional to J^m, with $1 \le m \le 3$, since J_L depends on $S1^m$. For a given set of values of x and Re, it was found experimentally that m does not depend significantly on either x or Re. In all conditions, we may consider $J_L \propto J^m$, with a relative precision that increases when the diffusion control of the wall reaction increases, and J can be estimated by measuring m at any point of observation for each value of Re through the relation

$$J \propto J_L^{1/m}. \tag{24}$$

Model and Algorithm for Numerical Analysis

In the two limiting cases of slow and fast diffusion of the LH· radical, the flux J of substrate to the wall is described by a set of linear differential equations that allow one to analyze the experimental data using a linear first-order reaction rate relative to H_2O_2. The flux data J derived from the measured J_L according to Eq. 24 are thus fitted as a simple approximation to this linear model.

The flux J in laminar flows is described by the following equations

$$D_{MS} \frac{\partial^2 S}{\partial y^2} - VS = 0; \quad x = 0; \quad -e < y < 0 \tag{25}$$

$$D_{LS} \frac{\partial^2 S}{\partial y^2} - \frac{4yC_m}{r} \frac{\partial S}{\partial x} = 0; \quad x < 0; \quad 0 < y < r \tag{26}$$

$$J(x) = D_{LS} \left(\frac{\partial S}{\partial y}\right)_{0+} = D_{MS} \left(\frac{\partial S}{\partial y}\right)_{0-}; \quad x > 0; \quad y = 0 \tag{27a}$$

$$D_{MS} \left(\frac{\partial S}{\partial y}\right)_{-e} = 0; \quad x > 0; \quad y = -e \tag{27b}$$

$$D_{LS} \left(\frac{\partial S}{\partial y}\right)_{r} = 0; \quad x > 0; \quad y = r \tag{27c}$$

$$S(y) = 1; \quad x < 0; \quad -e < y < r, \tag{27d}$$

where V is the phenomenological first-order rate fitting the data for $J = J_L^{1/m}$.

We assume that in turbulent flows the first-order rate, V, is still applicable. The error introduced by this assumption is, however, larger than in the laminar case since the flux of substrate diffusion to the interface is larger and the diffusion control is smaller in the turbulent case. Eq. 26 for bulk diffusion in the liquid phase must be replaced. Shaw and Hanratty (10) and Son and Hanratty (11) have shown that the substrate concentration profile for a turbulent liquid in a cylindrical tube could be described to a good degree of accuracy by the following relations that describe the diffusion process by a phenomenological diffusion coefficient $\tilde{D}(y)$

$$\tilde{D}(y) = D_{LS} + 0.00032 \, y^4 U_0^4 / \nu^3 \tag{28}$$

U_0 is the friction velocity related to the wall velocity gradient G by

$$G = U_0^2 / \nu. \tag{29}$$

The equation describing the substrate concentration profile in the liquid phase is then

$$\frac{\partial}{\partial y}\left[\left(\frac{1}{S_c} + 0.00032 \frac{y^4 U_0^4}{\nu^3}\right)\frac{\partial S}{\partial y}\right] - \frac{U_0^2}{\nu} y \frac{\partial S}{\partial x} = 0, \tag{30}$$

where S_c is the Schmidt number, $S_c = \nu/D_{LS}$. In stationary conditions, both for laminar and turbulent flows, J should also be equal to the

substrate consumption by the enzyme

$$J = \int_{-\epsilon}^{0} V S(y)\, dy. \tag{31}$$

A finite difference scheme was always used for the integration of the differential equations established above (6, 17). The discretion scheme and the required approximations are given in Appendix II. The concentration profiles of the substrate for two typical values of *Re*, 500 (laminar) and 5,000 (turbulent), are given in Fig. 4 for two different values of *V*. If the diffusion layer, δ, is defined as the distance from the gel-water interface to the point where ($S1 - S$) decreases to a value equal to 10% of

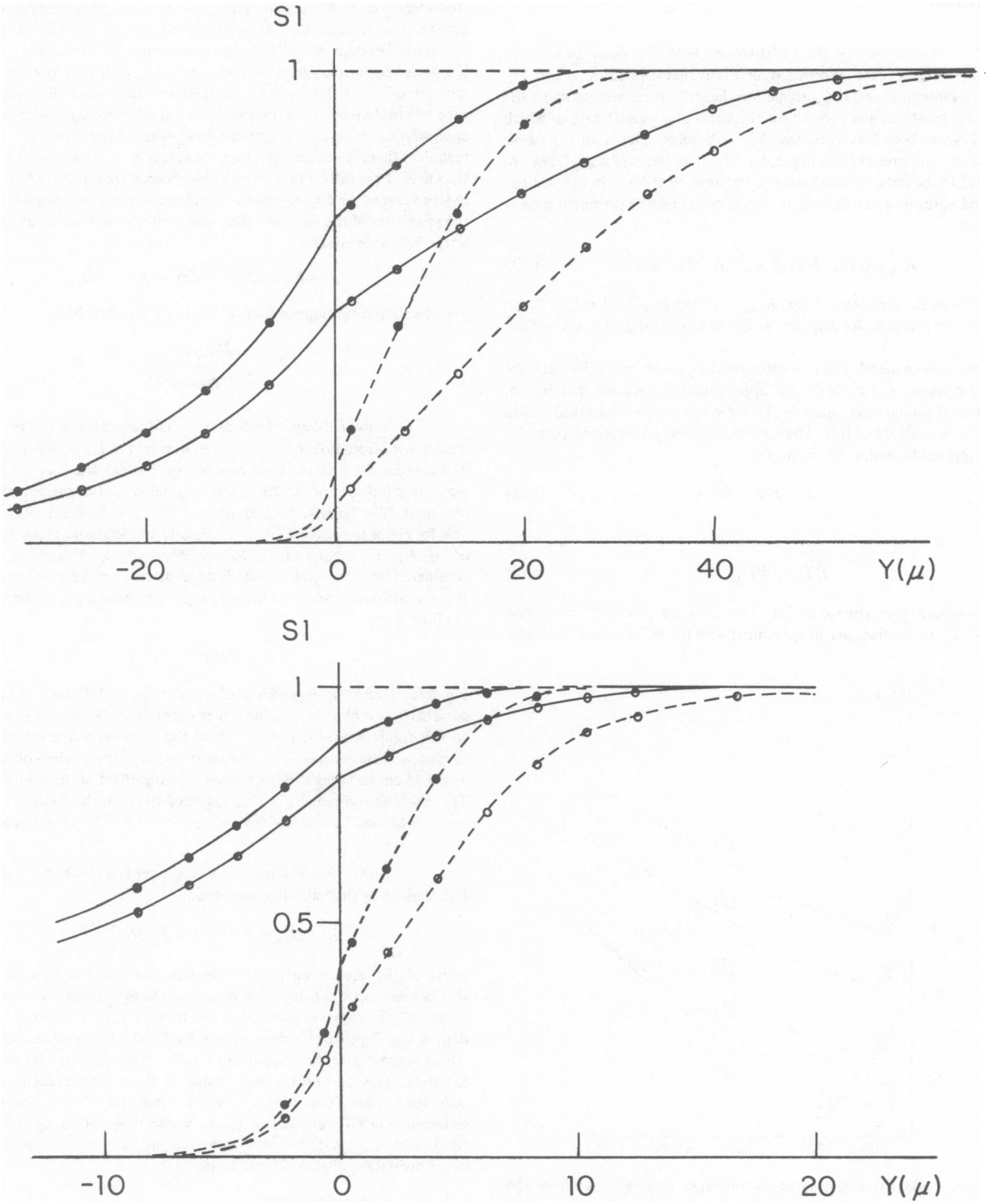

FIGURE 4 Substrate concentration profiles at $Re = 500$ (*top*) and 5,000 (*bottom*) for $V = 7.4\ s^{-1}$ (---) and $0.074\ s^{-1}$ (—) at $x = 0.3$ cm (●) and 3 cm (○). The data correspond to $D_{LS} = 5 \times 10^{-7}\ cm^2/s$, $D_{MS} = 2.5 \times 10^{-7}\ cm^2/s$, $r = 0.28$ cm. According to Eq. 34, the two values of *V*, $7.4\ s^{-1}$ and $0.074\ s^{-1}$ correspond to $ET = 1.36 \times 10^{-3}$ cm/s and 1.36×10^{-4} cm/s, respectively.

($S1 - S0$), δ appears to be much smaller in turbulent than in laminar flow and in no case larger than a few hundredths of millimeter. δ is thus always much smaller than the radius of the tube. It is thus licit to assume, as in the section Diffusion Convection of a Substrate at a Liquid-Solid Interface, a constant velocity gradient throughout δ and also to reduce the cylindrical problem to a two-dimensional one (parallel and perpendicular to the flow). In such conditions, three main aspects of the calculations can be discussed.

Consistency of the Calculations with the Ideal Case. In some cases an analytical expression for J is available (ideal case, e.g., Eq. 4 for the laminar case). Our calculations have been carried out using the general expressions given above for the particular (ideal) case in which the gel water boundary equation, $S0 = 0$, holds. The results of these calculations are presented in Fig. 5, for $S1 = 1$ in terms of K_{ideal}. They are identical to the data corresponding to the analytical Eq. 4 in the laminar case and agree also to this analytical expression for the turbulent case at the input

$$K_{ideal} = 0.116\, D_{LS}^{2/3}\, x^{-1/3} r^{-2/3}\, \nu^{1/3} Re^{7/12} \qquad (32)$$

and far from the input ($x > 5$ cm) $K_{ideal} = 0.0645\, D_{LS}^{2/3}\, r^{-1}\, \nu^{1/3}\, Re^{7/8}$. No analytical expressions for K_{ideal} are available in the range $0.2 < x < 5$ cm (11).

In the more general situation corresponding to the enzymated gel, the two estimations of J given by the approximations, Eq. B8 and B10 of Appendix II should be compatible. They have been found identical within 3% in all investigated cases. The simple following expressions were also found applicable, within 3% accuracy,

$$J = ET \cdot S0 \qquad (33)$$

where

$$ET = (VD_{MS})^{1/2} \qquad (34)$$

is the first-order enzymatic activity rate constant in $cm \cdot s^{-1}$ for a unit surface. These relations are in agreement with the calculations of Blaedel et al. (20) who characterize the reaction rate of an uniformly enzymated membrane of infinitely large thickness. This is confirmed by the value of S at the gel-glass interface, which is found lower than $10^{-2}\, S1$ in all cases.

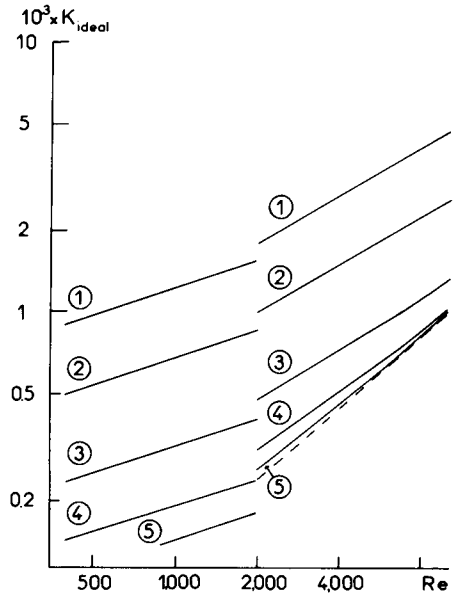

FIGURE 5 Ideal flux computed for different Reynolds numbers and positions along the tube ($r = 0.28$ cm, $l = 3.5$ cm, $e = 0.02$ cm, $D_{LS} = 5 \times 10^{-7}$ cm²/s, $D_{MS} = 2.5 \times 10^{-7}$ cm²/s). The dashed line (---) corresponds to a fully developed turbulent flow. $x = 50$ μm, (*1*); 300 μm, (*2*); 0.28 cm, (*3*); 1.28 cm, (*4*); and 3.28 cm, (*5*).

Transport Coefficient, K. The transport coefficient K was defined above by Eq. 5. Fig. 6 shows that K is always larger than the theoretical values, K_{ideal}, and smaller than $1.2\, K_{ideal}$, in agreement with the general inequalities, Eq. 6b, given above for the laminar case. The difference between K and K_{ideal} increases when ET decreases, i.e., for a less active enzymated gel with lower control by diffusion. It exceeds 15% only for $ET < 1.4\ 10^{-4}$ cm·s⁻¹ for turbulent flows near the input of the tube where J must be maximum. Such a small difference with the ideal case, which is expected for laminar flows, was not reported previously for turbulent flows. It means that, even for values of $S0$ as high as $0.5\, S1$, the thickness of the diffusion layer, which is proportional to D_{LS}/K, is almost independent of the activity of the enzymated surface and depends only on the properties of the flow. We may thus write, with good accuracy, for a linear first-order system

$$J \approx K_{ideal}\,(S1 - S0) = ET \cdot S0 \qquad (35b)$$

and the simple relation between J, $S1$, and ET thus holds

$$J \approx \frac{K_{ideal}\, S1}{1 + K_{ideal}/ET}. \qquad (36)$$

x and Re Dependence of J. The dependence of J on Re and x calculated from Eq. 36 for two different values of ET is shown in Fig. 7. The comparison with the ideal case in Fig. 5 shows one that the slope of log J as a function of log Re is always smaller and decreases when ET decreases. The laminar-to-turbulent transition is, however, still observable for ET as low as 3.10^{-4} cm·s⁻¹. Finally, in the laminar case, the slope of log J as a function of log Re increases with x. This slope may be considered as a constant, n, which depends only on the enzyme activity ET, the position x, and the laminar (n_{lam}) or turbulent (n_{turb}) character of the flow, and

$$J = J_0 Re^{n(ET,x)}. \qquad (37)$$

Fig. 8 illustrates this dependence of n_{lam} and n_{turb} on ET at $x = 0.3$ and 3.3 cm where most observations have been carried out. We have also reported on this figure maximal estimations of the error on n due to the 5-mm resolution of the optical fiber. They correspond to the n values obtained at $x + 0.25$ cm and thus eliminate any averaging effect of the circular fiber. The resulting error on ET is thus expected to be much smaller than 15% at $x = 3$ cm and 60% at $x = 0.3$ cm for $ET < 10^{-3}$ cm/s) (see below).

Light Flux Analysis. Combining Eqs. 24 and 37, the light flux is given by the following expression

$$J_L = J_{Lo} Re^{m \cdot n(ET,x)} = J_{Lo} Re^{n'(ET,x)} \qquad (38)$$

which allows one to analyze the experimental data within an accuracy that depends upon the degree of control of the light emission reactions by diffusion. The measurements of m and of n' (ET,x), altogether with the data of Fig. 7, permit the derivation of n (ET,x) and the estimation of ET which characterize the effective first-order system giving the best fit to the data. This accuracy which is due to the approximations used, is reflected by the values of $S0(x)$ calculated from ET. Finally, four distinct estimations of ET were derived for the values of n_{lam} (0.3), n_{lam} (3.3), n_{turb} (0.3), and n_{turb} (3.3) and thus from the measurement under different experimental conditions (Tables II and III).

DISCUSSION

The various values of the enzymatic activity rate constant ET, derived from this pseudo–first-order model appear

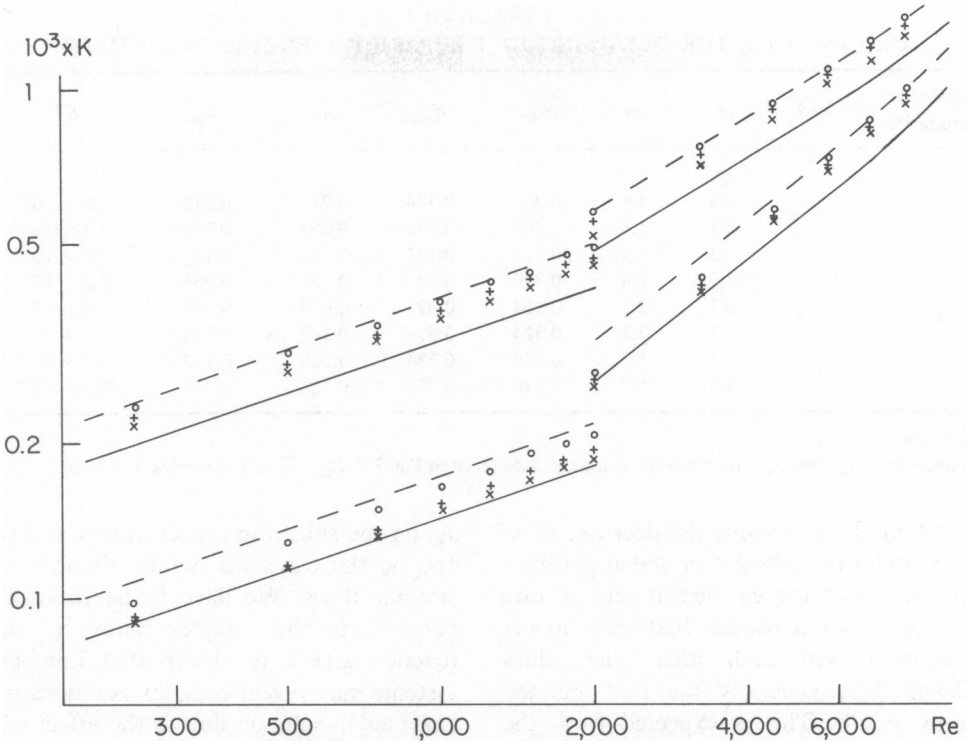

FIGURE 6 Comparison of the ideal transport coefficients with those corresponding to various values of ET (1.36×10^{-4} [o]; 5.44×10^{-4} [+], and 1.36×10^{-3} [x] cm/s). Dashed lines (---) correspond to the theoretical values of K obtained in the case of a constant flux to the wall ($K = 1.2\ K_{ideal}$). $D_{LS} = 5 \times 10^{-7}$ cm²/s.

rather consistent with each other. The error introduced by the approximations, as estimated from the ratio $S0/S1$, is clearly smaller for the most active tubes for which an upper limit in laminar flows can be set at ~35%.

Most of the effects described in the Results section are well predicted by the model. (*a*) When x increases, n' increases in laminar conditions. In particular, the effect described above in turning over the tube 2 corresponds to a large increase (from 0.3 to ~7 cm) of the abscissa x of observation. Similarly, the increase of n' at the laminar-to-turbulent transition is higher at $x = 3.3$ cm than at $x = 0.3$ cm. This is due, in fact, to the decreasing substrate wall concentration in the direction of the flow and thus to an increase of diffusion control. In particular, when x is small the ideal flux at the wall in turbulent conditions may be sufficiently high as compared with $ET \cdot S0$ that the order $n_{turb}(ET,x)$ could be smaller than $n_{lam}(ET,x)$ (see Fig. 8 for

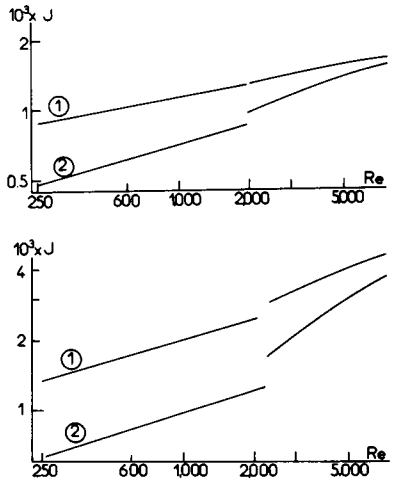

FIGURE 7 Theoretical dependences of J for two values of ET (*top*, 2.72 $\times 10^{-4}$ cm/s, *bottom*, 1.36×10^{-3} cm/s) for two positions $x = 0.28$, (*1*), and $x = 3.28$ cm, (*2*), as a function of *Re*.

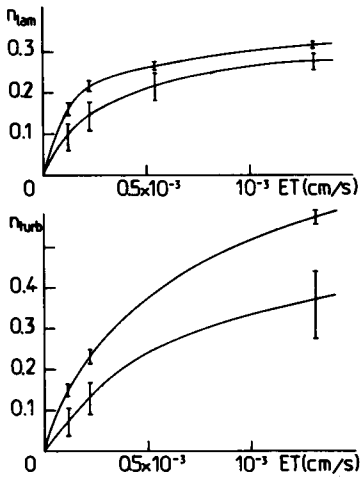

FIGURE 8 Effect of ET on n_{lam} (*top*) and n_{turb} (*bottom*) at $x = 0.3$ (*lower* curve) and $x = 3.3$ cm (*upper* curve) obtained by Eqs. 37 and 38. The bars correspond to the maximal error on n due to the 5-mm spacial resolution of the fiber (see text for explanation).

TABLE III
ANALYSIS OF n' FOR OBTAINING ET THE PARIETAL ENZYMATIC ACTIVITY*

Tube number	Mode of preparation	pH	x	m	n'_{lam}	n'_{turb}	n_{lam}	n_{turb}	ET‡	ET_2
			cm							
1	I	8	0.3	1.6	0.34	0.344	0.21	0.215	5×10^{-4}	4.3×10^{-4}
			3.3	1.6	0.405	0.541	0.255	0.338	4.5×10^{-4}	4.0×10^{-4}
2	I	8	0.3	1.4	0.255	0.182	0.182	0.13	3.2×10^{-4}	2×10^{-4}
			3.3	1.4	0.330	0.365	0.236	0.261	3.2×10^{-4}	2.6×10^{-4}
2	I	9.5	0.3	2.2	0.164	0.091	0.0745	0.041	8×10^{-5}	6×10^{-5}
			3.3	2.2	0.324	0.076	0.147	0.0345	10^{-4}	4×10^{-5}
3	II	8	0.3	1.7	0.220	0.224	0.129	0.132	1.7×10^{-4}	2.0×10^{-4}
			3.3	1.7	0.350	0.376	0.206	0.221	2.2×10^{-4}	2.0×10^{-4}

*In cm · s^{-1} per surface unit.
‡EI_1 and ET_2 are obtained from n_{lam} and n_{turb}, respectively, using the data given in Fig. 7: $D_{LS} = 5 \times 10^{-7}$ cm^2/s, $n = n'/m$.

$ET < 2 \times 10^{-4}$ cm/s). This explains the decrease of n' observed at $x = 0.3$ cm for the tube 2 operated at pH 9.5.

(*b*) The various values of the enzymatic activity rate constant, ET, derived from our pseudo–first-order model appear rather consistent with each other. The values obtained at x =0.3 cm differ generally from that obtained at x = 3.3 cm by <25%. This is expected from the relatively low effect of the spacial resolution of the fiber on the measured value of n', which is due both to its averaging effect and to the low dependence of n on x (see above).

(*c*) The apparent decrease of $d(\log J_L)/d(\log Re)$ observed in Fig. 3 and in Table I when $S1$ increases over 10^{-4} M may have two origins. The concentration of H_2O_2 in the gel could reach a large value as compared with the phenomenological Michaelis constant in Eq. 8 and make the first-order approximation inadequate. The first-order approximation, on the other hand, could require parameters for the best fit that may change with $S1$, though this change should not be very large in the range $S1$ to 3 $S1$ described in Table I.

The values of ET derived at pH 8 for each tube varies from 10^{-4} to 4.10^{-4} cm·s^{-1} depending upon the mode of binding of the enzyme to the gel. According to Eq. 34 and assuming that D_{MS} is independent of the tube since the composition of the gel is constant, the effective specific volume activity, V, introduced in Eq. 25, can be, therefore, ~16 times larger for the tubes obtained by covalent binding of the protein than for those obtained by entrapment of the enzyme. Finally, the experiments carried out on the same tube (n° = 2) at pH 8 or 9.5 show one that the chemiluminescent activity is much stronger at the lower pH value, as observed in solution (20–22).

CONCLUSION

This work was initiated to analyze quantitatively the light flux, J_L, in terms of diffusion convection and intrinsic enzymatic rate. This immobilized enzyme system, which is well adapted to spatial analysis, exhibits two apparently contradictory properties, the dependence of the light flux, J_L, on the substrate concentration in $S1^m$, with $m > 1.5$, and on the Reynolds number in $Re^{n'}$, with $n' > 0.3$ in laminar flows. We have found the explanation for this behavior in the complex nature of the light-emission reaction and have shown that immobilized enzymatic systems may reveal complex reactions more clearly than enzymes in solution due to the effect of diffusion of the various compounds, substrate and intermediate(s), involved in the overall reaction. The phenomenological relation (Eq. 24), $J_L = J^m$, which solves the contradiction mentioned above, is a consequence of both the nature of the chemiluminescent reaction and the high diffusion control of the enzymatic reaction catalyzed by immobilized peroxidase.

The first-order approximation proposed for the quantitative analysis of the system appears to yield consistent results in spite of the rather indirect relationship of the light emission rate, J_L, with the substrate flux, J, at the interface. In all instances, the accuracy of the results should be better for the more active tubes, and the covalent binding mode of the enzyme to the gel, introduced in these experiments, appears as an important improvement as compared with the entrapment method. The theoretical model predicts satisfactorily the effects visualized for the first time by immobilized enzymes, namely, the laminar-to-turbulent flow transition, the importance of the region of development of turbulent substrate concentration profiles, and fine positional effects due to the nonideal diffusion control in laminar flows.

This quantitative analysis has therefore provided insights both in the diffusion-convection phenomena and in the enzymatic process. Furthermore, we have shown that the enzymatic preparations are already sufficiently active to reveal the effect on the light flux of the distance to the input of the active tube and of the laminar or turbulent character of the flow. Preliminary investigations (7) have already shown that particular geometries, such as stenoses could also lead to a position-dependent light flux related to the local hydrodynamical properties of the flow. They have also shown the time dependence of J_L for nonstationary

flows. In particular, J_L decreases to 0 when the flow is stopped (7) and it is expected that the rate of this decrease depends on the enzymatic activity of the tube. Similarly, time-dependent responses of such systems are expected and have already been observed for periodical flows such as those for the blood circulation. The method thus appears to be an adequate model for the study of many aspects of the reactions of circulating substrates consumption of low molecular weight, which are catalyzed by enzymes located at the wall of blood vessels.

APPENDIX A

Eq. 6b should be considered within two limiting cases.

Limiting Case of a Constant Wall Concentration

The observed flux, $J(x_0)$ at $x = x_0$, should be compared with the theoretical flux, $J'(x_0)$, corresponding to a constant substrate wall concentration, $S0'(x)$ for $x < x_0$, equal to the observed concentration, $S0(x_0)$, at the position x_0. By applying Duhamel's theorem (5, 24), the substrate flux $J(x_0)$ is given for every wall conditions by

$$J(x_0) = -\int_0^{x_0} K_{ideal}(x_0 - \xi)\frac{dS0(\xi)}{d\xi}\,d\xi. \qquad (A1)$$

In the limiting case considered here, $-[dS0'(\xi)]/d\xi = [S1 - S0(x_0)]\delta(\xi)$, where $\delta(\xi)$ is the Dirac function centered at $x = 0$. Thus,

$$J'(x_0) = K_{ideal}(x_0)[S1 - S0(x_0)]. \qquad (A2)$$

The transport coefficient is thus simply K_{ideal} in this case. On the other hand, in our experimental conditions the wall concentration decreases from $S1$ at $x = 0$ to $S0(x_0)$ at $x = x_0$. $dS0(\xi)/d\xi$ is thus always negative. Furthermore, $K_{ideal}(x_0 - \xi)$ is an increasing function of ξ and $K_{ideal}(x_0 - \xi)\,dS0(\xi)/d\xi < K_{ideal}(x_0)\,dS0(\xi)/d\xi$ for each value of $0 < \xi < x_0$ and

$$J(x_0) > -\int_0^{x_0} K_{ideal}(x_0)\frac{dS0(\xi)}{d\xi}\,d\xi$$

thus,

$$J(x_0) > K_{ideal}(x_0)[S1 - S0(x_0)] \qquad (A3)$$

since $S0(0) = S1$. The first inequality is thus proven and Eq. A2 shows furthermore that the lower limit corresponds to a constant substrate wall concentration.

Limiting Case of a Constant Wall Flux

In reference 25 the relation between the wall flux, $J^*(x_0)$, assumed to be constant for $x < x_0$ and the wall concentration, $S0^*(x_0)$, at position x_0 has been shown to be

$$J^*(x_0) = \frac{2\pi}{3\sqrt{3}} K_{ideal}(x_0)[S1 - S0^*(x_0)] = 1.209\,K_{ideal}(x_0)[S1 - S0^*(x_0)]. \qquad (A4)$$

We want to show that the observed value of the wall concentration $S0(x_0)$ is smaller than the theoretical value $S0^*(x_0)$ corresponding to the case where $J^*(x_0) = J(x_0)$. Since the actual wall flux, $J(x)$, is a decreasing function of x, we have for every value of $x < x_0$, $J(x) > J(x_0) = J^*(x_0)$.

We define the new function $\bar{S} = S^*(x, y) - S(x, y)$. This function is a solution of the following system:

$$D_{LS}\frac{\partial^2\bar{S}}{\partial y^2} - \frac{4C_m y}{\nu}\frac{\partial\bar{S}}{\partial x} = 0 \qquad x > 0, y > 0$$

$$D_{LS}\frac{\partial\bar{S}}{\partial y} = J^*(x_0) - J(x)\ (<0) \qquad y = 0, x > 0.$$

According to the maximum principle (25), the minimal value, min $\bar{S}$ of $\bar{S}(x, y)$, is obtained either for $y = 0$ or for $x = 0$, $y > 0$. Setting $S0^*(x) = S^*(x, 0)$, if $S0^*(x) - S0(x)$ has a strictly negative minimum, this minimum can thus be obtained only at $y = 0$, $0 < x_1 < x_0$ since at $x = 0$, $S0^* = S0 = S1$. But $(\partial\bar{S})/(\partial y) < 0$ and for sufficiently small positive values of y, $\bar{S}(x_1, y) < \bar{S}(x_1, 0) = \min\bar{S}$, which is contradictory. We thus have $\min\bar{S} \geq 0$ and, in particular,

$$S0(x) \leq S0^*(x) \qquad (A5)$$

for $x \leq x_0$. Eq. A4 then leads to the following required inequality.

$$J(x_0) \leq 1.209\,K_{ideal}(x)\,[S1 - S0(x)]. \qquad (A6)$$

Eqs. A3 and A4 are equivalent to Eq. 6b in the text.

APPENDIX B

The scheme for discretion as well as the finite difference equations used in this work were established as follows.

Discretion Scheme

The diagram of discretion is that proposed by Gelif and Henry (6) (Fig. 9). The coordinates are thus: (*a*) in the gel phase, $x = ih_1$; $i = 1$ to N_1 with $N_1 h_1 = l$; $y = (j - 1/2)\,h_2 - N_3h_2$ with $j = 1$ to N_3 and $N_3h_2 = e$; (*b*) in the liquid phase, $x = ih_1$; $y = (j - 1/2)\,h_2 - N_3h_2$ with $j = N_3 + 1$ to N_2 and $N_2h_2 = e + r$. Furthermore, the dimension of h_2 has been choosen as 0.667 μm and 0.21 μm in the laminar and in the turbulent cases, respectively. The dimension of h_1 is 30 μm (laminar flow) and 10 μm (turbulent flow) at the input of the tube and is progressively increased as x increases. This discretion scheme is sufficient to lead to exact calculations (see the text). No mesh point has been taken at $y = 0$ since a smaller error is then expected (26).

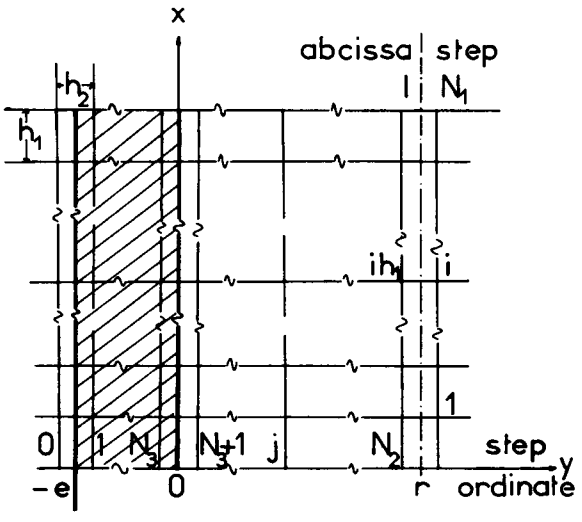

FIGURE 9 Discretion diagram used for the finite difference integration of the partial derivative equations.

Bulk Equations

The bulk Eqs. 25, 26, and 30 are approximated by the following relations

$$\text{Eq. 25:}\quad (D_{MS}/h_2^2)(s_{i,j-1} - 2s_{i,j} + s_{i,j+1}) - Vs_{i,j} = 0, \tag{B1}$$

where $s_{i,j}$ is an estimation of S at position (i, j).

$$\text{Eq. 26:}\quad (D_{LS}/h_2^2)(s_{i,j-1} - 2s_{i,j} + s_{i,j+1}) - \frac{4C_m(j - 1/2 - N_3)h_2}{h_1}(s_{i,j} - s_{i-1,j}) = 0 \tag{B2}$$

Eq. 30 may be more simply rewritten as

$$\frac{\partial}{\partial y}\left[A(y)\frac{\partial S}{\partial y}\right] - By\frac{\partial S}{\partial x} = 0 \tag{B3}$$

with $A(y) = 1/S_c + 0.00032\,U_0^4\,y^4/\nu^3$ and $B = U_0^2/\nu$. According to this notation the following approximation was used

$$(1/2\,h_2^2)\,|\,a_{j+1/2}(s_{i,j+1} - s_{i,j}) - a_{j-1/2}(s_{i,j} - s_{i,j+1}) + a_{j+1/2}(s_{i+1,j+1} - s_{i+1,j}) - a_{j-1/2}(s_{i+1,j} - s_{i+1,j-1})\,| - \frac{B(j - N_3 - 1/2)h_2}{h_1}(s_{i+1,j} - s_{i,j}) = 0 \tag{B4}$$

where

$$a_j = A[(j - N_3 - 1/2)h_2]. \tag{B5}$$

Boundary Conditions

The boundary equations (Eqs. 27b–27d) are approximated by the following equations: (*a*) at $y = -(N_3 - 1/2)h_2$ (gel-glass interface), $s_{i,0} = s_{i,1}$ for $i = 1$ to N_1; (*b*) at $y = r$, $s_{i,N_2} = s_{i,N_{2+1}}$ for $i = 1$ to N_1; (*c*) at $x = 0$, $s_{0,j} = 1$ for $j = 1$ to N_2. The equation of continuity, Eq. 27a, between the gel and liquid phases is assured by introducing the following values of $s_{i,j}$ at $j = N_3$ and N_{3+1}

at $j = N_3$ $s_{i,j+1}$ is replaced by

$$[(D_{MS} - D_{LS})s_{i,j} + 2D_{LS}s_{i,j+1}]/(D_{LS} + D_{MS}) \tag{B6}$$

at $j = N_{3+1}$ $s_{i,j-1}$ is replaced by

$$[2D_{MS}s_{i,j-1} + (D_{LS} - D_{MS})s_{i,j}]/(D_{LS} + D_{MS}). \tag{B7}$$

Eq. A6 is equivalent to the replacement of $s_{i,N_{3+1}}$ by the value theoretically obtained at this position if the gel was extended to $j = N_{3+1}$. Eq. A7 is equivalent to the replacement of s_{i,N_3} by the value theoretically obtained at this position if the liquid phase was extended to $j = N_3$.

Calculation of the Enzymatic Reaction Rate of Substrate Consumption

The flux $J(x)$ as calculated from the wall concentration gradient (Eq. 27a) is approximated by

$$J(ih_1) = 2\,D_{LS}[s_{i,N_{3+1}} - S0(ih_1)]N_3/e, \tag{B8}$$

where the concentration $S0$ at the gel-water interface is approximated by

$$S0(ih_1) = s_{i,N_3} + 1/2\,(s_{i,N_3} - s_{i,N_{3-1}}). \tag{B9}$$

The flux J as calculated from the enzymatic reaction rate (Eq. 31) is approximated by the following equation

$$J(ih_1) = \frac{eV}{N_3}\left\{\sum_{j=1}^{N_{3-1}} s_{i,j} + [3\,s_{i,N_3} + S0(ih_1)]/4\right\}. \tag{B10}$$

The Particular Ideal Case[1]

Similar calculations have also been performed to obtain the substrate flux, J_{ideal}, occurring when the specific enzymatic rate is so high that the wall concentration, $S0$, is negligible as compared with the bulk concentration $S1$. In this case the system of equations describing the gel phase has to be replaced by the more simple boundary equation, $S0 = 0$ for all x values.

We are greatly indebted to Professor J. M. Lhoste (U. 219 Institut National de la Santé et de la Recherche Médicale, Institut Curie, F-91405 Orsay, France), Professor J. P. Kernevez (Université de Technologie, F-60206 Compiègne, France) for helpful discussions and to Dr. J. Henry (INRIA, F-78153 Le Chesnay, Cédex, France) for the demonstration reported in Appendix A and B.

Received for publication 13 January 1983.

REFERENCES

1. Nakache, M., and P. Peronneau. 1979. Relationship between hydrodynamic forces and vascular wall phenomena. II. Study of the influence of friction on the parietal microenvironment by the fixed enzyme method. *Biorheology.* 16:265–276.
2. Wingard, L. B., E. Katchalski-Katzir, and L. Goldstein. 1976. Applied Biochemistry and Bioengineering. Vol. 1. Immobilized Enzyme Principles. Academic Press, Inc., New York. 359.
3. Wingard, L. B., E. Katchalski-Katzir, and L. Goldstein, 1979. Enzyme Technology. Academic Press, Inc. New York. 2:303.
4. Horvath, C., and B. A. Solomon. 1972. Open tubular heterogeneous enzyme reactors: preparation and kinetic behavior. *Biotechnol. Bioeng.* 14:885–914.
5. Kobayashi, T., and K. J. Laidler. 1974. Theory of the kinetics of reactions catalyzed by enzymes attached to the interior surfaces of tubes. *Biotechnol. Bioeng.* 16:99–118.
6. Gellf, G., and G. Henry. 1975. Experimental and theoretical study of diffusion, convection and reaction phenomena for immobilized enzyme systems. *In* Analysis and Control of Immobilized Enzyme Systems. D. Thomas and J. P. Kernevez, editors. North Holland Publishing Co., Amsterdam. 253–275.
7. Dimicoli, J. L., M. Nakache, and P. Peronneau. 1982. Direct visualization of diffusion convection phenomena at liquid solid interfaces by the use of a chemiluminescent enzymatic immobilized system. *Biorheology.* 19:281–300.
8. Freeman, T. M., and W. R. Seitz. 1978. Chemiluminescence fiber optic probe for hydrogen peroxide based on luminol reaction. *Anal. Chem.* 30:1242–1246.
9. Cormier, M. J., and P. M. Prichard. 1968. An investigation of the mechanism of the luminescent peroxidation of luminol by stopped flow techniques. *J. Biol. Chem.* 243:4706–4714.
10. Shaw, D. A., and T. J. Hanratty. 1977. Turbulent mass transfer rates to a wall for large Schmidt numbers. *AIChE. J.* 23:28–37.
11. Son, J. S., and T. J. Hanratty. 1967. Limiting relation for the eddy diffusivity close to a wall. *AIChE. J.* 13:689–696.
12. Vogel, G. E., O. K. Johannson, F. O. Stark, and R. M. Fleischmann. 1967. The chemical nature of the glass coupling agent interface. *Proceedings of the 22nd American Technological Conference of the Society of the Plastics Industry.* 13b:1–10.

[1]See references 11 and 16.

13. Weston, P. D., and S. Avrameas. 1971. Proteins coupled to polyacrylamide leads using glutaraldehyde. *Biochem. Biophys. Res. Commun.* 45:1574–1580.
14. Cotton, H. B., and H. B. Dunford. 1973. Studies on horseradish peroxidase. XI. On the nature of compounds I and II as determined from the kinetics of the oxidation of ferrocyanide. *Can. J. Chem.* 51:582–587.
15. Krindel, P., and A. Silberberg. 1979. Flow through gel-walled tubes. *J. Colloid Interface Sci.* 71:39–50.
16. Peronneau, P., and M. Nakache. 1979. Relationships between hydrodynamic forces and vascular phenomena. I. Measurement of parietal friction by pulse type Doppler velocimeter. *Biorheology.* 16:257–263.
17. Levich, V. 1962. Convective diffusion in liquids. *In* Physicochemical Hydrodynamics. N. R. Amundson. Prentice-Hall Inc., Englewood Cliffs, New Jersey. 112–116.
18. Schmith, G. D. 1979. Parabolic equations. *In* Numerical Solutions of Practical Differential Equations: Finite Difference Methods. J. D. Crank, H. G. Martin, and D. M. Melluish, editors. Clarendon Press, Oxford. 1–74.
19. Strother, G. K., and E. Ackerman. 1961. Physical factors influencing catalase rate constants. *Biochim. Biophys. Acta.* 47:317–326.
20. Blaedel, W. J., T. R. Kissel, and R. C. Bogulaski. 1972. Kinetic behavior of enzymes immobilized in artificial membranes. *Anal. Chem.* 44:2030–2037.
21. Strehler, B. L. 1968. Bioluminescence assay: principles and practice. *In* Methods of Biochemical Analysis. D. Glick, editor. Interscience, New York. 99–181.
22. Brolin, S. E., E. Borglund, L. Tegner, and G. Wettermark. 1971. Photokinetic microassay based on dehydrogenase reactions and bacterial luciferase. *Anal. Biochem.* 42:121–135.
23. Hodgson, E. K., and I. Fridovich. 1973. The role of O_2^- in the chemiluminescence of luminol. *Photochem. Photobiol.* 18:451–455.
24. Myers, G. E. 1971. Superposition. *In* Analytical Methods in Conduction Heat Transfer. McGraw-Hill, Inc., New York. 151–166.
25. Protter, M. H., and H. F. Weinberger. 1967. Parabolic equations. *In* Maximum Principle in Differential Equation. Prentice-Hall Inc., Englewood, Cliffs, NJ. 159–195.
26. Henry J. 1978. Contrôle d'un réacteur enzymatique á l'aide de modèles à paramètres distribués. Ph.D. thesis, Université de Paris, Paris, France. 277.